INTERFEROMETRIC PROCESSING OF PALSAR WIDE-BEAM SCANSAR DATA

Charles Werner, Urs Wegmüller, Othmar Frey, Maurizio Santoro

Gamma Remote Sensing AG, Worbstrasse 225, CH-3073 Gümligen, Switzerland,
http://www.gamma-rs.ch, cw@gamma-rs.ch

ABSTRACT

Processing of ScanSAR data for interferometric applications requires careful attention to the phase and position accuracy to obtain interferometric products with high correlation and continuous phase across the bursts. We describe an interferometric processing system developed for ScanSAR data acquired by the ALOS PALSAR instrument able to produce differential interferometric products with 350 km swath width that are without visible phase discontinuities between ScanSAR beams.

1. INTRODUCTION

Between 2006 and 2011 the ALOS PALSAR acquired an impressive archive of ScanSAR data which are potentially suited also for SAR interferometry. The advantage of ScanSAR is the ability to achieve wide-swath coverage required for short repeat intervals with moderate increase of system complexity. Interferometry based applications are facilitated by wide swath widths permitting short repeat intervals and the potential for frequent acquisitions to reduce measurement errors due to atmospheric and ionospheric phase variability. ScanSAR successively illuminates parallel overlapping swaths with a burst of radar pulses. A sketch of the PALSAR acquisition modes is shown in Figure 1.
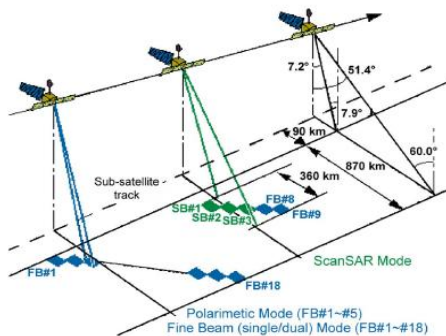

Figure 1: PALSAR Acquisition Modes

Table 1: PALSAR ScanSAR WB1 Mode Parameters

Center Frequency (MHz)	1270
Chirp Bandwidth (MHz)	14
Polarization	HH
Incidence angle (deg.)	18 – 43.3
Swath Width (km)	350
Data Rate (Mbps)	120
PRF(Hz) swath dependent	1669 - 2315
Pulses per Burst swath dependent	247 - 355, 327

To access the high potential of the PALSAR ScanSAR archive we implemented a methodology for PALSAR ScanSAR raw processing and interferometry. In the following we explain the methodology used and show examples for both ScanSAR – Stripmap and ScanSAR – ScanSAR interferograms.

This work is also of interest in the context of the planned Sentinel-1 [1] which will operate primarily using the Interferometric Wide-Swath mode.

2. PALSAR SCANSAR CHARACTERISTICS

The PALSAR instrument operates in several modes including Stripmap single and dual-pol fine-beam (FBS, FBD), Quad-Pol (POL), and ScanSAR (WB1, WB2) as shown in Figure 1. The ScanSAR mode predominately used by PALSAR was WB1 with characteristics as shown in Table 1. ScanSAR operates by progressive illumination of overlapping swaths to build up the wide-swath. In the case of PALSAR, the illumination of each beam is for approximately 0.17 seconds. Each of the 5 beams has a different pulse repetition frequency (PRF) determined by the range and azimuth ambiguity constraints. The number of pulses in each burst varies due to the differing PRFs.

The time that a point on the ground can be illuminated by the antenna, called the aperture time, determines the number of bursts that an echo from this point can be received and processed. For ScanSAR beam 4 the

aperture time is about 3.45 seconds equivalent to 7345 pulses. With a burst interval of 0.16 seconds, a point on the ground will be illuminated for approximately 20 bursts.

3. PROCESSING SCANSAR DATA

ALOS PALSAR ScanSAR mode data are acquired in both ascending and descending orbits. Particularly, the data in descending orbits are of interest as this configuration is rarely covered by Stripmap mode acquisitions. The PRF and starting slant range change in discrete steps during the acquisition. In our approach we resample the data to a constant PRF along track which facilitates the subsequent processing. In the case of ScanSAR data rather than resampling each track to the its own nominal PRF value, we typically resample all the data of the 5 beams to the same constant PRF value. Often we chose the nominal PRF of the continuous strip-map data acquired by ALOS PALSAR using beam 4, 2150.5 Hz, for this purpose. The data are synchronized to a common time and spatial reference grid such that the images from the different beams fall onto the grid in azimuth and slant-range.

In our processing chain a phase-preserving Range-Doppler (RD) SAR processor is used for image formation. This approach was proposed for processing XSAR and Radarsat data [3][4] and has also been implemented for PALSAR [7][8]. The time between the bursts is filled with 0.0 and the data processed as one continuous strip. It should be noted that since the inter-burst time is not an integral number of inter-pulse periods (1/PRF), resampling of the data to a constant PRF preserves phase coherence between the bursts.

Alternate processing of ScanSAR data has been performed using the SPECAN and extended SPECAN algorithms that efficiently process each individual burst with some increase of complexity in the algorithm [5][6]. One of the significant advantages of the zero-fill RD approach is that we can make use of existing proven software for image formation, autofocus optimization, and interferogram generation.

Another advantage of zero-fill RD is the possibility of direct generation of ScanSAR-Stripmap interferograms. The SLC image produced from the ScanSAR data after zero filling is identical in format to the Stripmap images. Since it has been resampled to the same PRF as the Stripmap image, generation of the interferogram proceeds as with strip-mode images.

What is different about ScanSAR is that the azimuth resolution has been significantly reduced due to the fact that each beam is illuminated only approximately 20% of the time in order to obtain a wider image swath. The processing approach described here requires as much computation during azimuth compression as if the data

had been continuous but obtains an image that is accurate with respect to phase, geometry, and radiometry.

3.1. Mosaicking ScanSAR beams and geocoding

The SLC images are produced at the same pixel spacing of 9.4 meters in range and 3.1 meters in azimuth as strip-map images. The actual azimuth resolution is reduced, as expected, by a factor of approximately 5 to about ~60 meters. The SLC image from each beam is corrected for the range antenna pattern as supplied by NASDA.

The SLC data are detected and multi-looked, e.g. using 3 range looks and 16 azimuth looks, to produce multi-look intensity (MLI) images of each beam. The resulting MLI images produced by zero-fill strip-map processing have no visible azimuth scalloping due to burst timing [4].

These image strips can be mosaicked without interpolation to form the full 5-beam mosaic. This is possible because of the resampling of the raw data to a common slant-range and azimuth grid.

Intensity offsets between the beams may be corrected by matching the average intensity in the overlap region between beams. The accuracy of the matching depends on accurate knowledge of the range antenna patterns and noise level due to azimuth ambiguities and thermal noise.

3.2. Terrain geocoding of the image mosaic

The full mosaic of the MLI images is then terrain geocoded using the SRTM DEM or other DEM if available. For the purposes of terrain geocoding of the SAR image, the image can be processed without azimuth burst synchronization to maintain full resolution (see below).

One of the products of the terrain geocoding is the DEM height resampled to the slant range coordinates of the MLI mosaic. Performing the geocoding refinement on the full mosaic avoids DEM offsets between the individual beams.

3.3. Burst Synchronization for DINSAR

A critical factor in processing ScanSAR data for repeat-track interferometry is synchronization of the bursts [3][4]. A requirement for interferometric coherence is that the scene is viewed from the same azimuth aspect angle by corresponding pulses in the two tracks. Therefore, coherence is improved by nulling out echoes in the corresponding bursts of the two tracks that do not overlap spatially. In order to maintain high coherence, the region of the raw data bursts that do not overlap are set to 0 as part of the resampling and zero-fill

processing. Note that for ScanSAR-Stripmap interferometry, there is always 100% overlap (100% of the available ScanSAR burst time), but the raw data of the strip-map image should be nulled out for the region between the bursts of the ScanSAR image to optimize the coherence [8].

The burst overlap is determined using the start and stop times of the burst in the two tracks, considering also the offset between the two reference times. Without specific measures to synchronize the bursts by adjusting satellite timing or trajectory, the chance of having tracks with burst overlap > 1/2 is only about 20% for a ScanSAR with 5 beams. In our approach the burst synchronization can be checked without actually processing the data.

3.4. Differential interferogram formation

The full swath DEM in radar coordinates (slant range) is sliced into the individual beams and used in the SLC co-registration, using an algorithm that takes into account the local terrain height to avoid decorrelation and phase errors due to misregistration. Each ScanSAR beam is individually resampled to the matching beam in the second acquisition.

The differential interferograms are calculated from the co-registered SLCs which were produced using burst synchronization. A simulated interferometric phase is calculated based on the terrain heights and the orbit data assuring full phase consistency between the different beams. These 5 differential interferograms are mosaicked without requiring interpolation since the SLC data use a common geometrical reference. No further phase adjustment is required between the differential interferograms in the full differential interferogram mosaic.

4. PROCESSING EXAMPLES

The first example shown is a ScanSAR – Stripmap (FBS) differential interferogram over Los Angeles. (Figure 2). Except for the sea surface high coherence is observed for almost the entire area thanks to a short baseline, relatively short time interval, and low vegetation density. The second example shows a ScanSAR - ScanSAR differential interferogram over California, covering the dates 20061231 and 20070402. These two ScanSAR acquisitions were acquired with different PRFs with the result that the burst synchronization varies strongly along-track and is an excellent test of the burst-synchronization algorithm. Burst overlap begins at 0.47, increases to 1.0 (perfect overlap) and then drops to 0.0 along the track. Differential interferograms from all 5 swaths were mosaicked into a single differential interferogram in slant-range geometry and subsequently geocoded into geographic coordinates as shown in Figure 3.
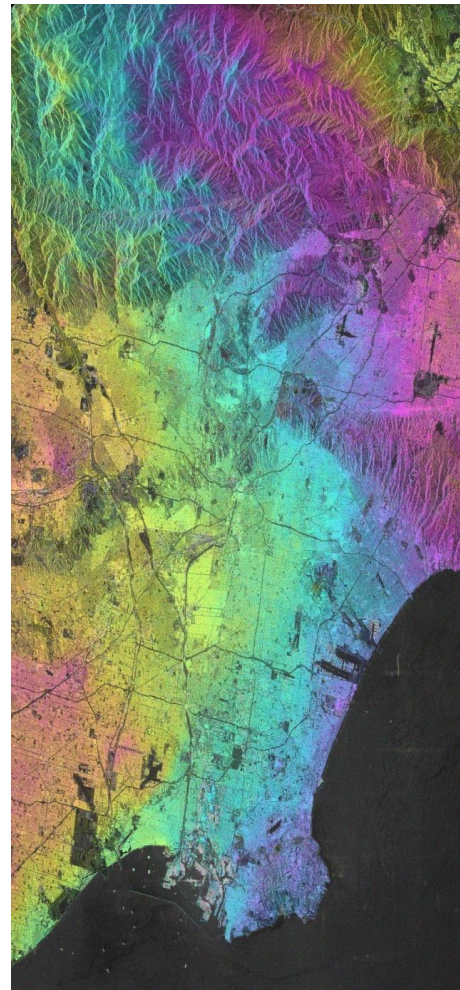

Figure 2: PALSAR ScanSAR - FBS differential interferogram (shown in SAR geometry) over Los Angeles, FBS on 20070702, ScanSAR WB1 on 20061231, $B_\perp = 148m$, dt = $184days$, using SRTM as height reference.
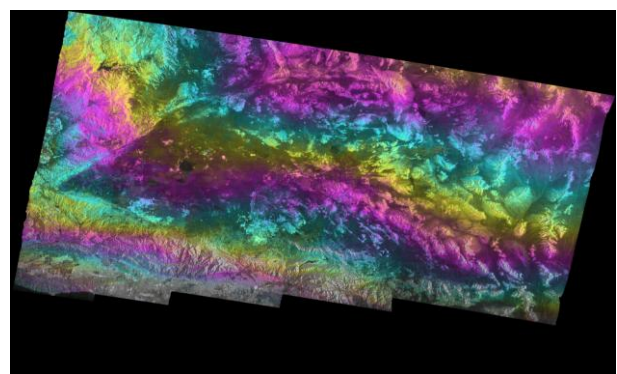

Figure 3: ScanSAR - ScanSAR differential interferogram over California. 20061231 – 20070402, $B_\perp = 482m$, dt = $92days$, using SRTM as height reference. The burst overlap varies over the image (see text). The image extends over all 5 PALSAR ScanSAR WB1 beams.
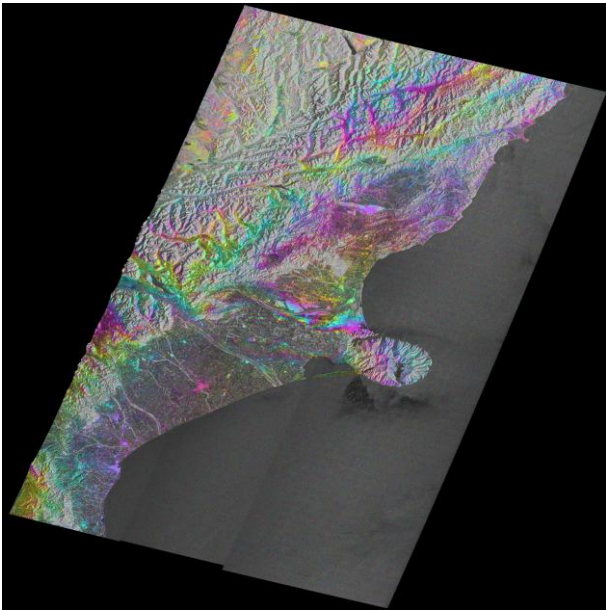
Figure 4: Differential Interferogram over New Zealand 20071020 , 20101028. Track is 361km long and swath width is 250 km for beams 1,2,and 3. Image projection in geographic coordinates.
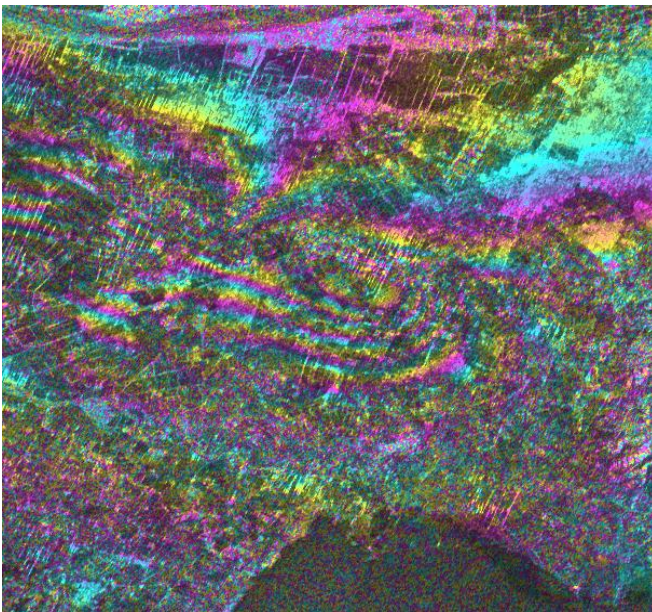

Figure 5: Earthquake related deformation fringes. Each fringe represents 11.8cm motion along the line of sight.

The next example shown is a PALSAR WB1 ScanSAR - ScanSAR pair covering the magnitude 7.0 earthquake that occurred west of Christchurch, New Zealand, on 20100903 (UTC). The burst overlap varied from close to 1.0 at the start of the track then decreased to 0.75 at end. The New Zealand PALSAR WB1 ScanSAR - ScanSAR interferometric pair, 20071020 - 20101028, has a perpendicular baseline of about 1490 meters
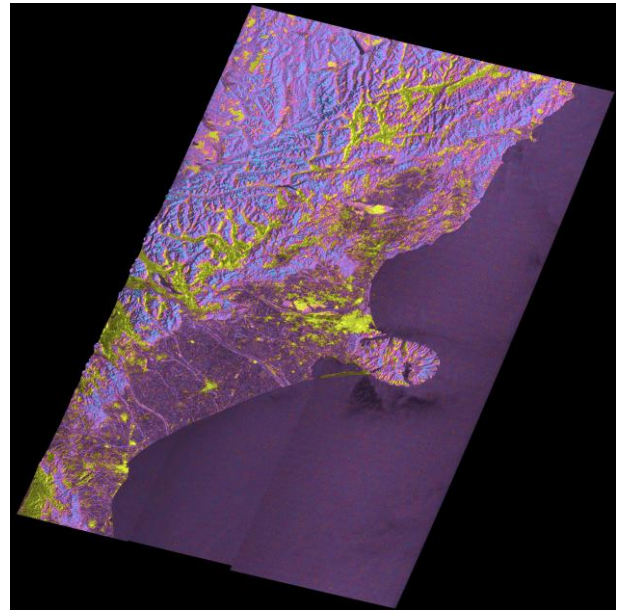

Figure 6: New Zealand interferometric correlation of interferogram shown in Figure 4.

(Figure 4). Significant fringes from the co-seismic movement are clearly visible in the expanded region located near the image center, see Figure 5. This differential interferogram shows reasonable correlation despite a 3 year time interval, especially for urban areas. The corresponding interferometric correlation is shown in Figure 6.

5.   CONCLUSIONS

An interferometric processing system for ScanSAR data was introduced and ALOS PALSAR ScanSAR – Stripmap and ScanSAR – ScanSAR differential interferograms were shown. The processing system uses a common slant-range and azimuth grid for the raw and SLC data and considers burst synchronization and related common band filtering to optimize the coherence and to get phase consistent SLC and interferogram products. The processed SLC images and interferograms exhibit high coherence, phase consistence between the different beams and a high geometric accuracy.

Such processing shall support further exploration of the existing very rich ALOS PALSAR data archive. Furthermore, the development can be understood as a preparation for Sentinel-1 that will use an interferometric ScanSAR mode as its main mode of operation.

6.   REFERENCES

[1] De Zan, F., Guarnieri, A., Rocca,F., "Advances in SAR interferometry for Sentinel-1 with TOPS,"

IEEE Radar Conference 2008, 26-30 May 2008 Rome doi::10.1109/RADAR.2008.4720871

[2] Rosenqvist, A, Shimada, M., Watanabe M., "ALOS PALSAR: A Pathfinder Mission for Global-Scale Monitoring of the Environment," *IEEE Transactions on Geoscience and Remote Sensing*, vol. 45, no. 11, Nov. 2007, pp. 3007-3316 doi: 10.1109/TGRS. 2007.901027.

[3] Bamler, R, and Eineder, M, "ScanSAR processing using standard high precision SAR algorithms", *IEEE Transactions on Geoscience and Remote Sensing*, January 1996 vol. 34 pp. 212-218, doi: 10.1109/36.481905.

[4] Holzner, J., and Bamler, R., "Burst mode and ScanSAR Interferometry,", *IEEE Transactions on Geoscience and Remote Sensing*, vol. 40, no. 9, Sep. 2002, pp. 1917-1931.

[5] R. Lanari, Hensley,S.,and Rosen, P., "Modified SPECAN algorithmfor ScanSAR data processing," in *Proc. IGARSS*, Jul. 1998, vol. 2, pp. 636–1517.

[6] A. Bertran Ortiz, Zebker, H., "ScanSAR-to-Stripmap Mode Interferometry Processing Using ENVISAT/ASAR Data," *IEEE Transactions on Geoscience and Remote Sensing*, vol. 45, no. 11, Nov. 2007, pp. 3468 - 3480.

[7] Liang, C., et al. ALOS PALSAR "ScanSAR Interferometry and its Application in Wenchan Earthquake", *ESA Fringe Workshop 2009*.

[8] Sandwell, D., Mellors, R., and Tong, X., "ScanSAR Interferometry with PALSAR", *3rd ALOS Joint PI Symposium, Kona, Hawaii*, Nov. 9-13, 2009.

7.   ACKNOWLEDGEMENT